Journal of Catalysis **186,** 334–344 (1999)
Article ID jcat.1999.2574, available online at http://www.idealibrary.com on

Stability of the Square-Planar Cu^{2+} Sites in ZSM-5: Effect of Preparation, Heat Treatment, and Modification

A. V. Kucherov, A. N. Shigapov,* A. A. Ivanov,† and M. Shelef

*Scientific Research Laboratory, Ford Motor Company, MD 3179/SRL, P.O. Box 2053 Dearborn, Michigan 48121; *Institute of Chemistry of Natural Organic Materials, Krasnoyarsk, Russia; and †Zelinsky Institute of Organic Chemistry, RAS, Moscow, Russia*

Received January 27, 1999; revised May 24, 1999; accepted May 24, 1999

HZSM-5 with $SiO_2/Al_2O_3 = 50$ into which 0.5 wt% Cu (Cu/Al ~ 0.25) was introduced after the removal of extralattice Al species by basic or acidic treatment shows no inhibition of the irreversible loss of active, tetrahedrally coordinated Cu^{2+} sites upon thermal treatment. Removal of the extralattice Al coupled with a complete exchange of all Brønsted groups for Cu^{2+} cations results in a noticeable stabilization of the reactive square-planar sites. FTIR data confirm the absence of free Brønsted groups in the exchanged samples. Quantitation of "ESR-visible Cu^{2+}" in these exchanged samples, calcined at 500–800°C in air, gives values of 1.8 and 1.65 wt% for base-treated and acid-treated samples, respectively. These values are near the limit of exchange assuming a Cu/Al = 1 stoichiometry in this high-silica material. Formation of aggregated copper species is of minor importance, and the majority of Cu^{2+} remains well isolated and contributes to the ESR signal. It is evident from the comparison of partially exchanged and completely exchanged samples that one part of Cu^{2+} ions inhibits the irreversible loss of another portion of Cu^{2+} quite efficiently. Also, a strong stabilizing effect is noted for samples prepared on acid-pretreated zeolite containing 0.5 wt% Cu and additional Mg^{2+} cations. Here a large part of the copper ions (>50%) preserves the parent square-planar Cu^{2+} state even after calcination at 800°C. The effect of La, Ca, or Sr is also observable but less pronounced. Both the acidic pretreatment and the introduction of an appropriate amount of Mg^{2+} ions contribute to the better stabilization of the most reactive part of Cu^{2+} cations in CuMgZSM-5. Magnesium ions compete with Cu^{2+} for the cationic positions replacing first the less reactive, pyramidal Cu^{2+} cations. An increase in the Mg^{2+} loading results in a decrease in the number of the reactive cupric sites in samples calcined at 500–550°C but simultaneously improves further the thermal stability of the square-planar Cu^{2+} ions. © 1999 Academic Press

INTRODUCTION

The stability of the cupric ions in square-planar coordination in ZSM-5 zeolites is of considerable interest since it was repeatedly shown that these are the most reactive catalytic sites in oxidation reactions and probably also in NO_x selective reduction (1–3). These cationic sites are vulnerable to irreversible deactivation, in particular at elevated temperatures in the presence of water vapor. The cupric ions in the square-planar coordination have a distinct, easily identifiable signature in the ESR spectrum which serves as a direct indicator of the efficacy of various stabilizing methods. The effects of various treatments and modifications on the stability are quantifiable by measuring the ESR spectra with reference to those of frozen solutions of dilute Cu^{2+} ions (2). It was demonstrated earlier that La oxide markedly attenuates the spatial rearrangement of the cupric active sites in ZSM-5 in the less reactive state (3). The stabilizing effect of Mg oxide on ZSM-5 was also noted before (4, 5). This work is an extension of these investigations.

EXPERIMENTAL

Sample Preparation

Samples containing only Cu (mono-cationic) and those containing Cu with a modifying cation (bi-cationic) were prepared by ion-exchange or impregnation of treated or untreated HZSM-5 zeolite by copper and by introduction of other ions—La, Mg, Ca, and Sr. The same HZSM-5 zeolite, having a Si/Al ratio of 50 and crystallinity >90% (PQ Corporation), was used for preparation of all the samples under investigation.

The intent of the base or acid pretreatments was to remove extra-framework aluminum species formed during calcination, and also removal of amorphous impurities. The alkaline treatment was carried out as follows: the NH_4-form of original ZSM5-zeolite was calcined at 550°C for 2 h and at 575°C for 30 min. The calcined sample (20 g) was treated with 1 L of 0.15 M solution NaOH at 80°C for 1.5 h. The obtained solid was filtered and washed with distilled water, dried, and then ion-exchanged back to the NH_4 form with a saturated solution of NH_4Cl. In some samples this procedure was repeated.

The acidic treatment was carried out as follows: the original NH_4ZSM-5 was calcined at 550°C for 2 h and at 575°C for 20 min. Calcined zeolite (15 g) was treated with 1 L of 0.1 M solution of nitric acid at 80°C for 2 h. The treated zeolite was washed thoroughly with distilled water and dried at 120°C overnight. To obtain HZSM5-HNO_3-twice, 6 g of this

0021-9517/99 $30.00

material was calcined at 575°C for 2 h and at 600°C for 2 h. The solid was treated with 1 L of 0.1 M solution of nitric acid at 80°C for 2 h. The treated zeolite was washed thoroughly with distilled water and dried at 120°C overnight.

To prepare Cu-exchanged samples, 1 g of material, after acidic or alkaline treatment, was contacted with a solution of 10 g $Cu(NO_3)_2 \cdot 3H_2O$ in 20 mL of distilled water and washed with distilled water. Then the procedure was repeated and Cu-exchanged zeolites were calcined at 500°C for 2 h. To prepare exchanged samples with other cations (La, Mg) the same procedure was followed, using corresponding water solutions of the nitrates.

Bicationic samples containing 0.5 wt% Cu and modified by La, Mg, Ca, and Sr were made by consecutive incipient wetness impregnation (0.8 cc/1 g) of the NH_4- or H-forms of the zeolite by water solutions of corresponding nitrates with subsequent drying and calcination at 500°C. In the sequence of the preparation copper was introduced first, followed by modifier. Since the introduced amount of ions was retained by the impregnated samples no further analysis was done. The ion-exchanged samples were those containing 1.65 and 1.8 wt% Cu. They were made by twofold exchange of base-treated and acid-treated HZSM-5.

Surface Area and Porosity

Texture properties of parent and modified samples were studied by low-temperature adsorption–desorption of N_2. Surface parameters were measured on aliquots of ∼200 mg using a Micrometrics ASAP 2400 instruments. The samples were evacuated at 350°C for 6 h.

ESR Measurements

The stability of the reactive square-planar Cu^{2+} sites in different samples was monitored by ESR (3, 6). The ESR spectra, at 20°C and −196°C, were taken, for samples evacuated after thermal treatment in air, in the X-band on a Bruker ESP300 spectrometer, equipped with a cavity st8410.91. The Bruker ESP300E software and the special Bruker program WIN-EPR (version 901201) were used for the data treatment (baseline correction, double integration, and subtraction) of the recorded spectra. The ESR signals of Cu^{2+} were registered in the field region 2000–4000 G (10 scans with a sweep time of 42 s). For a more accurate measurement of the ESR parameters and evaluation of relative concentration of square-planar Cu^{2+}, the $g_{\parallel}$-part of the spectra was registered separately (field region, 2650–3250 G; modulation amplitude, 4.0 G; microwave power, 6.41 mW; 10 scans with a sweep time of 42 s).

The samples were pressed without binder and crushed into 0.1- to 0.2-mm particles. Then sample charges (48–52 mg) were placed in identical quartz ampoules (3.5 mm diameter), calcined in a furnace at a given temperature, taken out, immediately connected to the vacuum system, evacuated for 2–3 min to 0.03 Torr, and sealed off. Then the spectra were registered at 20°C and normalized for the differences in sample weight.

Frozen water solutions of copper(II) nitrate with 0.625, 0.25, and 0.1 wt% Cu were used as standards for the measurement of the absolute number of cupric ions in zeolitic samples by ESR. The spectra were taken at −196°C for weighed samples of approximately equal volume placed in the same quartz ampoules. Freezing the solutions produces solid specimens with isolated Cu^{2+} ions closely approximating the CuHZSM-5 zeolite saturated with H_2O (7). Therefore, for direct quantitative comparison, copper-containing samples were impregnated with water and the ESR spectra were taken at −196°C. For highest accuracy, all sets of samples were measured consecutively, with ampoules positioned in the same position inside the ESR resonator.

FTIR Spectroscopy

IR spectra were recorded in the transmittance mode using a Mattson Galaxy 4326C FTIR spectrometer. The samples (∼4–10 mg) were pressed onto gold grids to form IR-transparent specimens, put into the spectrometer, and evacuated at 450°C for 6 h. The properties of Brønsted and Lewis acid sites (BAS and LAS) and other centers were studied by using acetonitrile-d_3 as a molecular probe (8).

RESULTS AND DISCUSSION

Surface Area and Porosity

Table 1 summarizes the surface area and porosity data of some of the examined samples. The data in the table encompass surface areas derived from the BET and Langmuir isotherms and porosity measurements by the BJH (Barrett, Joyner, Halenda) method which distinguishes the surface area and pore volume associated with pores of >17 Å diameter and the same parameters associated with micropores smaller than that. The micropores encompass the channels of the ZSM-5 zeolite. It is seen that both basic and acidic treatment of the parent zeolite causes only negligible changes in either the surface area or the porosity of the HZSM-5 (samples 1–3, 6, 7). Introduction of 0.5 wt% Cu into the zeolite (sample 4) leads to a small change in microporosity without a measurable loss of surface area. However, introduction of the maximum amount of Cu by ion exchange (sample 5; 1.8 wt% Cu) lowers both porosity and surface area.

Introduction of both Mg^{2+} ions by ion exchange and Cu^{2+} by impregnation (sample 9; 0.7 wt% Mg + 0.5% Cu) causes an even higher loss of surface area and porosity. It is important to note, however, that subsequent severe thermal treatment of this sample (750°C, 2 h) does not cause any further change in the properties of this Mg-containing sample (compare samples 9 and 10). On the other hand, the

TABLE 1

Surface Area and Porosity of Examined Samples

	Sample's description	BET area (m^2/g)	Langmuir area (m^2/g)	Surface area (m^2/g)		Pore volume (cm^3/g)		
				BJH desorption	Micropores	17–3000 Å BJH desorption	Micropores	Single point total
1	HZSM-5	425.2 ± 7.4	571.0 ± 5.3	135.1	241.7	0.429	0.111	0.464
2	HZSM-5–NaOH	432.5 ± 7.6	579.4 ± 6.0	141.7	233.7	0.550	0.106	0.555
3	HZSM5–NaOH-twice	438.7 ± 7.5	589.9 ± 5.9	161.0	247.3	0.503	0.112	0.547
4	Cu(0.5)HZSM-5–NaOH	423.2 ± 6.7	568.4 ± 6.6	143.4	221.3	0.507	0.101	0.527
5	Cu(1.8)ZSM5–NaOH	399.4 ± 5.8	536.6 ± 6.3	133.6	223.9	0.425	0.103	0.446
6	HZSM-5–HNO_3	424.9 ± 7.4	569.8 ± 6.2	128.9	251.0	0.439	0.114	0.465
7	HZSM-5–HNO_3-twice	429.3 ± 8.0	575.9 ± 5.8	129.5	250.9	0.520	0.114	0.505
8	Cu(0.5)HZSM5–NaOH (750°C, 2 h)	372.5 ± 3.1	501.3 ± 9.6	165.7	181.5	0.569	0.084	0.564
9	Cu(0.5)MgZSM5–NaOH	360.1 ± 5.4	483.5 ± 5.5	115.6	202.8	0.466	0.093	0.478
10	Cu(0.5)MgZSM5–NaOH (750°C, 2 h)	363.7 ± 3.6	489.1 ± 8.1	138.8	193.2	0.477	0.090	0.493

Note. The samples were calcined at 500°C for 2 h (except Nos. 8 and 10).

monocationic samples show substantial loss of the surface area and porosity as a result of an identical thermal treatment (compare samples 4 and 8).

FTIR Measurements

(1) The influence of HZSM-5 pretreatment with NaOH. The FTIR spectra of the hydroxyl region for HZSM-5 zeolites before and after basic treatment exhibit intensive hydroxyl stretches at 3610 and 3745 cm^{-1} which are characteristic of bridging Si–(OH)–Al hydroxyls representing Brønsted acid sites (BAS) and isolated silanol Si–OH groups on surface defects, respectively (8). A peak at 3660 cm^{-1} could be tentatively assigned to Al–OH hydroxyls on extraframework aluminum species. The intensity of the OH stretching bands and the ratio of intensity of silanol and bridged OH groups are only slightly lowered after basic treatment.

The properties of the surface acidic sites were measured in much greater detail by using acetonitrile-d_3 as a molecular probe: the ν(CN) stretching adsorption band in the IR spectrum is very sensitive to the interaction between this molecule and the acid sites (8–11). The adsorption was carried out at 100°C to suppress the formation of multidentate surface complexes with more than one BAS.

The difference spectra of CD_3CN adsorbed on HZSM-5 and HZSM-5 treated by base are shown in Figs. 1 and 2. After the first doses of CD_3CN are adsorbed the intensity of the band corresponding to BAS (3610 cm^{-1}) decreases. Simultaneously, new bands at 2795, 2420, and 1690 cm^{-1} appear due to hydrogen bond formation. These bands form an ABC triplet originating from Fermi resonance between the stretching vibration, n(OH), and the first overtones of the bending vibrations, d(OH) and g(OH) (9). The calculation of the position of the center of gravity gives a shift of the band at 3610 cm^{-1} as $\Delta\nu_{OH} = 1140$ cm^{-1}. The basic treatment leads to some decrease in the intensity of the bands associated with the perturbed OH groups. The center of gravity of the ABC triplet does not change.

After adsorption of CD_3CN on HZSM-5, bands in the region of CD and CN bond vibrations appear. The fundamental $n_s(CD_3)$ and $n_{as}(CD_3)$ frequencies are at 2112 and 2250 cm^{-1}, respectively (9). Two main bands appear in the CN spectral region at 2327 and 2297 cm^{-1}. According to literature data (8, 9, 11), these bands can be attributed to the adsorption on LAS and BAS, respectively. The relatively high temperature of the adsorption prevented the formation of weaker adsorption complexes.

The dynamics of the intensity of the CN stretching bands shows that the surface complexes of CD_3CN with LAS are formed more easily than those of with BAS. The intensity of bands corresponding to CD_3CN–BAS complexes starts to increase significantly only after saturation of LAS by the acetonitrile.

Basic treatment of HZSM-5 does not cause significant changes in the IR spectra in the region of CN stretching. The kinetics of the growth of the bands associated with BAS and LAS shows that for base-treated HZSM-5 the preferential formation of CD_3CN surface complexes with LAS is clearer than in the untreated sample. At saturation the [BAS]/[LAS] ratio is 3.34 and 3.60 for untreated HZSM-5 and base-treated HZSM-5, respectively, pointing to some decrease in the relative LAS concentration as a result of the pretreatment. This treatment does not remove the LAS completely but more severe treatments were avoided since they result in the loss of lattice sites. Evacuation at 100°C leaves only strongly bound species on the surface, associated with the strong acidic sites. The [BAS]/[LAS] of the adsorbed complexes ratios are 1.62 and 1.50 for untreated HZSM-5 and base-treated HZSM-5, respectively.

(2) Base-treated CuZSM-5. The FTIR spectra of Cu-ZSM-5 systems in the region of OH stretching vibration are shown in Fig. 3. The intensity of the band at 3610 cm^{-1}

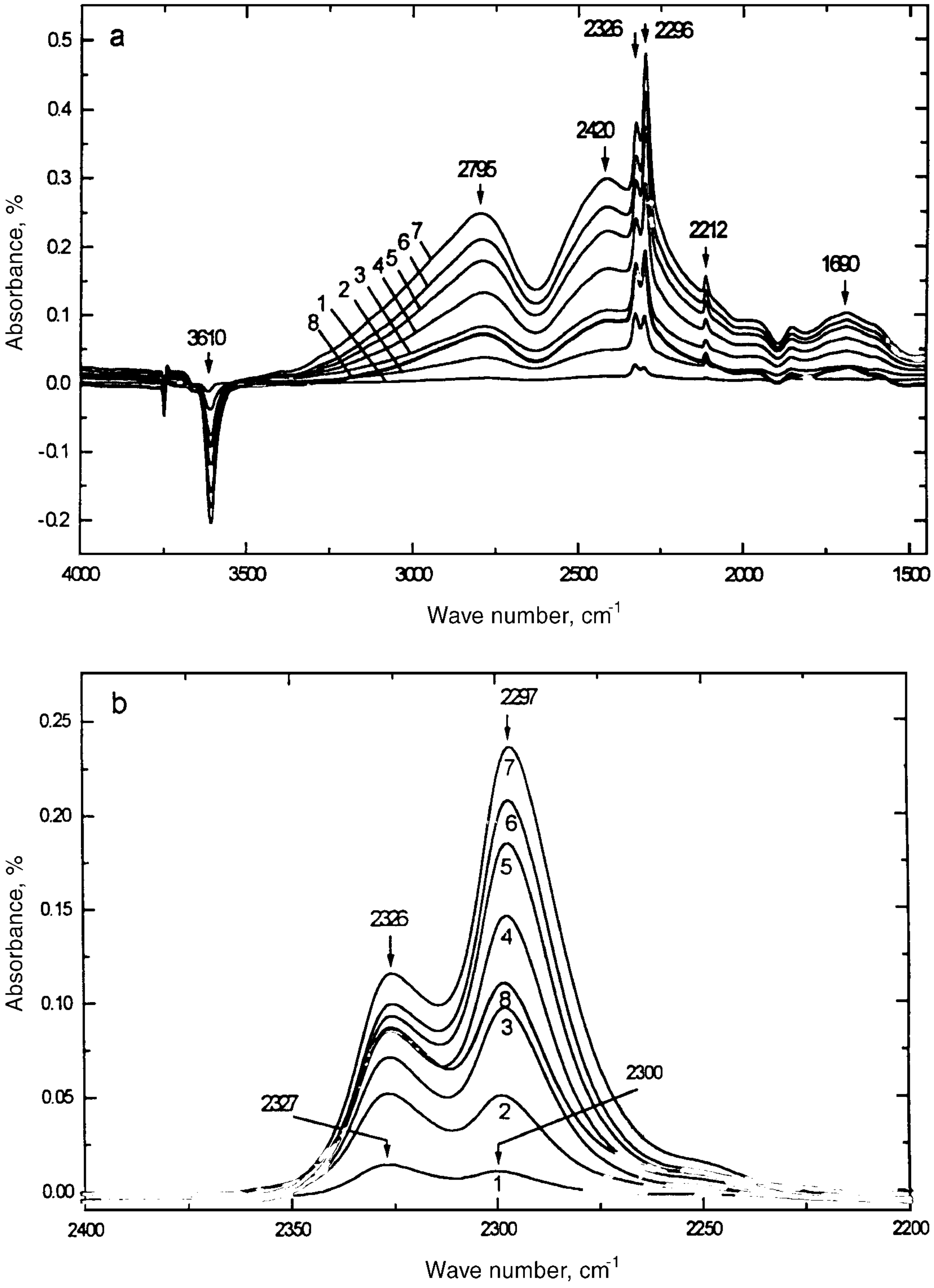

FIG. 1. Difference FTIR spectra of HZSM-5 (a) in the region of OH and (b) CN stretching vibration after adsorption of CD_3CN: (1) 0.1, (2) 0.2, (3) 0.35, (4) 0.45, (5) 0.55, (6) 0.65, (7) 1.2 $mmol/g_{cat}$, and (8) after evacuation at 100°C.

decreases noticeably after introduction of 0.5 wt% Cu, and the band disappears completely in the sample with ~1.8 wt% of Cu. These results confirm the ease with which the protons of BAS exchange with Cu^{2+} ions, leading to complete suppression of Brønsted acidity.

The difference spectra of CD_3CN adsorbed on CuZSM-5 are shown in Fig. 4 and compared with corresponding metal-free sample. The addition of 0.5 wt% Cu leads to disappearance of the C band (at 1685 cm^{-1}) of the ABC triplet. The calculation of the position of the center of gravity for

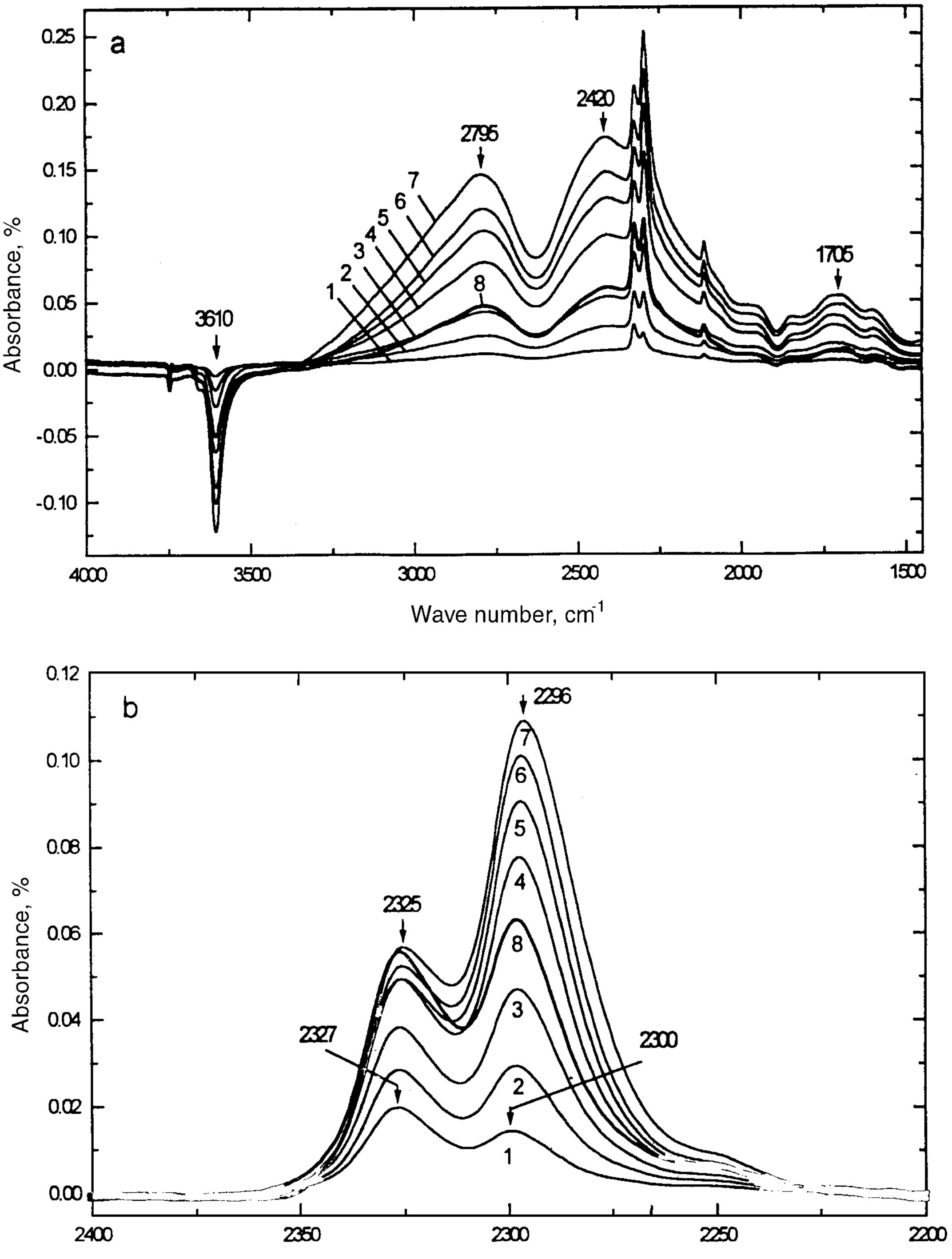

FIG. 2. Difference FTIR spectra of HZSM-5-NaOH (a) in the region of OH and (b) CN stretching vibration after adsorption of CD_3CN: (1) 0.1, (2) 0.2, (3) 0.35, (4) 0.45, (5) 0.55, (6) 0.65, (7) 1.2 mmol/g_{cat}, and (8) after evacuation at 100°C.

OH bands gives a shift of $\Delta\nu_{OH} = 1070$ cm^{-1} which points to a weakening of BAS acidity as compared with metal-free zeolite ($\Delta\nu_{OH} = 1150$ cm^{-1}). The increase in the Cu content leads to a decrease in the intensity of the perturbed OH groups in direct correspondence to the decrease in the concentration of bridged OH groups (Fig. 3).

In the region of the CN-bond vibration, three bands, at 2327, 2316, and 2297 cm^{-1} were observed after adsorption of CD_3CN on Cu(0.5)ZSM-5. The bands at 2327 and 2297 cm^{-1} were also observed for metal-free samples and were attributed to adsorption of CD_3CN on LAS and BAS, respectively. The ratios [BAS]/[LAS], after evacuation at

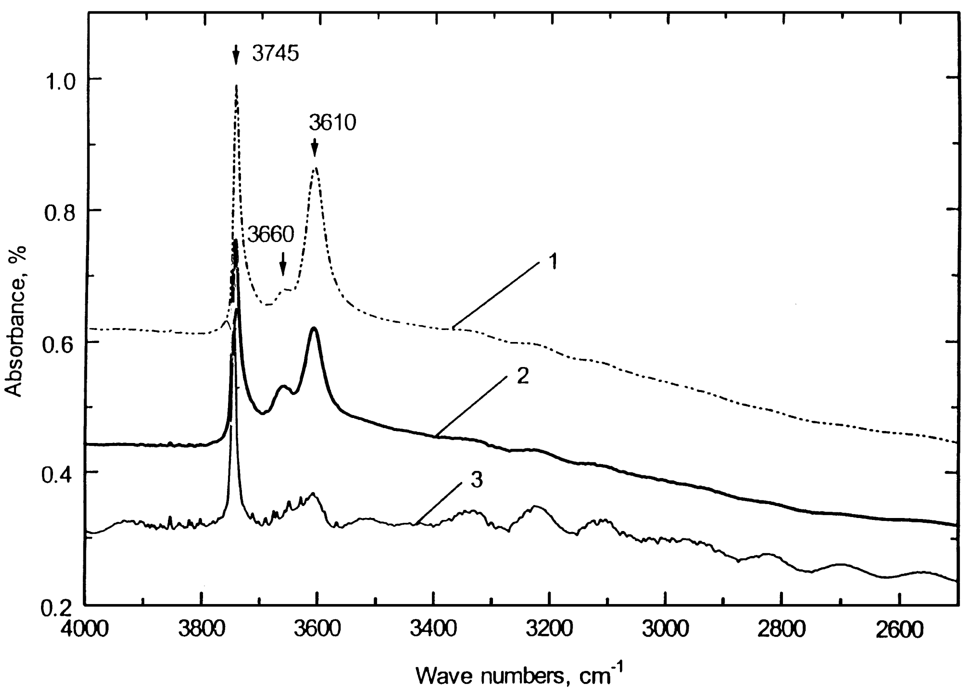

FIG. 3. FTIR spectra in OH stretching region of (1) HZSM-5–NaOH, (2) Cu(0.5)HZSM-5–NaOH, and (3) Cu(1.8)ZSM-5–NaOH calcined at 500°C.

100°C, are 9.37 and 5.27, respectively, for the Cu-containing and Cu-free samples. This is again points to some decrease in the concentration of LAS in Cu-containing zeolite as compared to the metal-free sample. The band at 2316 cm^{-1} could be associated with adsorption complexes of CD_3CN with Cu sites.

The increase in the concentration of copper to 1.8 wt% complicates the spectrum. After adsorption of acetonitrile only two bands of H-bonded OH groups at 2420 and 2840 were observed. The calculation of the shift of parent OH groups gives $\Delta\nu_{OH} = 975$ cm^{-1} which points to a further decrease in the acidic strength of residual BAS as compared to the metal-free and Cu(0.5)ZSM-5 samples.

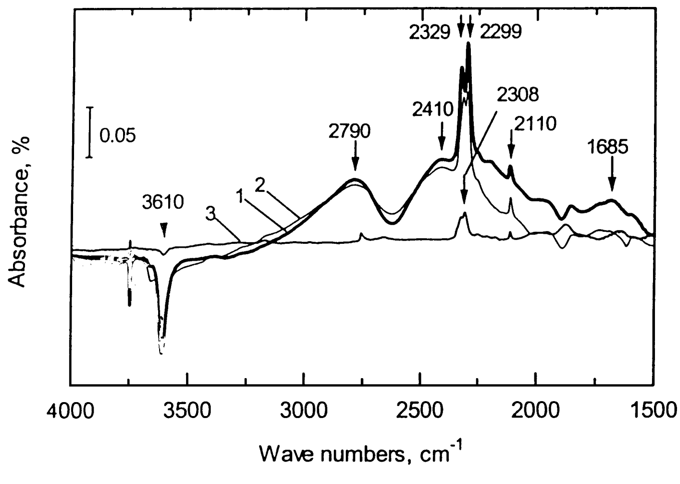

FIG. 4. Difference FTIR spectra of CD_3CN adsorbed on (1) HZSM-5–NaOH, (2) Cu(0.5)HZSM-5–NaOH, and (3) Cu(1.8)ZSM-5–NaOH after evacuation at 100°C.

In the region of CN stretching vibration the bands at 2345, 2327, 2310–2315, 2300, and 2210 cm^{-1} were observed. The band at 2327 cm^{-1} and a weak band which appeared at a high concentration of CD_3CN at 2300 cm^{-1} could be assigned to LAS and BAS, respectively. The assignment of the bands at 2345, 2310–2315, and 2210 is uncertain. The interpretation of Cu–CD_3CN IR spectra on samples containing Cu is, in our opinion, confounded by the possibility of chemical interaction between this organic molecule and the reactive Cu^{2+} species, especially at $T > 100$°C. It was shown, for example, that reduction of square-planar Cu^{2+} ions in CuZSM-5 by benzene occurs at room temperature (12). Reduction of copper sites by the test-molecule in this particular case also cannot be excluded, possibly affecting the spectra.

(3) CuMgZSM-5 samples. Addition of magnesium does not change significantly the IR spectrum in the region of the vibration of OH groups, as compared with Cu(0.5)ZSM-5. Adsorption of CD_3CN leads to the appearance of a doublet AB band at 2800 and 2425 cm^{-1}. The calculation of the maximum shift of the parent OH groups gives $\Delta\nu_{OH} = 1015$ cm^{-1}, indicating somewhat more acidic BAS as compared to monocationic CuZSM-5. It should be noted that the OH groups interact with acetonitrile molecules only at

high concentration of CD_3CN. Simultaneously, the bands at 3400 and 3145 appear as a result of interaction with weaker acidic sites.

Only one strong band at 2302 cm^{-1}, with a weak shoulder at 2325 cm^{-1}, was observed in the region of CN bond stretching vibration. This line cannot be assigned to a complex with BAS because it exhibits a high stability after evacuation at high temperatures. The position of the band at 2302 cm^{-1} is very close to the one reported for MgAlPO and MgY (2303–2305 cm^{-1} (13, 14)) and that observed in the CuZSM-5 sample after calcination (2300 cm^{-1}). The intensity of this band is twice as high as that found for the Cu-containing zeolite. Tentatively, the band could be assigned to the superposition of bands from CD_3CN–Mg and CD_3CN–Cu complexes. It is not possible to deconvolute the line into individual components.

(4) Influence of high-temperature treatment. Calcination at 700°C for 2 h destroys the BAS in HZSM-5 as evidenced by the sharp decrease in the intensity of bridged OH groups and the formation of the weak band at 3780 cm^{-1}, typical of the Al_2O_3 phase. A similar drop in BAS in partially exchanged Cu(0.5)HZSM-5 takes place upon calcination. At the same time, a new form of copper appears to be characterized by the band at 2300 cm^{-1} after adsorption complex formation with CD_3CN. The stretching vibration of the CN bond of CD_3CN on Cu^+ ions was observed at 2305–2300 cm^{-1} for Cu(I)ZSM-5 (11). It is worth noting that calcination of CuMgZSM-5 sample at 700°C does not lead to a significant change in the spectra of adsorbed acetonitrile. The spectrum of the CN stretching region is almost the same as that before calcination. In comparison with the monocationic sample it points, qualitatively, to a higher thermal stability of the cupric sites in the samples which also contain Mg.

ESR Measurements

(1) Quantitative results of ESR measurements. In the study of CuZSM-5 by ESR spectroscopy the intensity of the ESR signal is usually expressed in arbitrary units. Quantitation of the ESR-active fraction of the Cu^{2+} ions in the samples is, however, of crucial importance for the evaluation of the stability changes. For this, it is necessary to compare double integrals (DI/N) of the ESR spectra from CuHZSM-5 with an absolute Cu^{2+} standard whose intensity is measured under identical conditions. It was demonstrated earlier that frozen diluted solutions of inorganic Cu salts may be used as a reference, because in the solid state these salts form crystallohydrates with magnetically isolated cupric ions, and this separation by hydrate shells becomes even more effective in diluted water solutions (2, 18). In earlier studies $CuSO_4$, $CuCl_2$, and $Cu(NO_3)_2$ water solutions were successfully used (2, 18, 19). In the present work the measurement of zeolitic samples impregnated with water with reference to frozen $Cu(NO_3)_2$ solutions was used once more. To provide the maximum accuracy, ESR spectra were taken during one set of measurements at 77 K in a quartz Dewar filled with liquid nitrogen. The same ampoule, with a sample of the frozen solution of an identical packing height (10 ± 0.2 mm) was positioned exactly in the same place of the resonator.

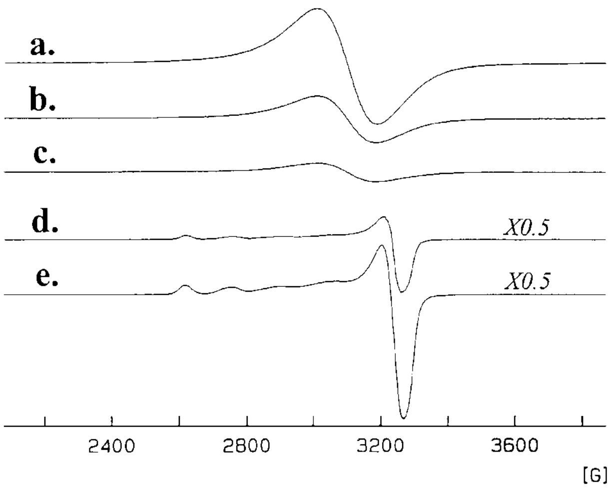

FIG. 5. ESR spectra, at 77 K, of frozen water solutions of $Cu(NO_3)_2$ ((a) 0.625 wt% Cu, 79 mg; (b) 0.25 wt% Cu, 77.7 mg; (c) 0.1 wt% Cu, 81.3 mg) and of two zeolitic samples impregnated with water ((d) Cu(0.5) HZSM-5, 34 mg; (e) Cu(1.8)ZSM-5, 33 mg).

Figure 5 shows the Cu^{2+} ESR signals from frozen solutions differing in Cu^{2+} concentration (a, b, c) and ESR spectra of two hydrated CuHZSM-5 samples (d, e) differing in both copper concentration and preparation method (impregnation and exchange). The shape difference between the first three spectra and the last two indicates that the magnetic separation of the cupric ions in the water-saturated zeolites is more effective than in the water itself. Signals d and e are identical in shape but differ substantially in intensity. These spectra, with $A_{\parallel} = 132$ G and $g_{\parallel} = 2.39$, indicate that the symmetry of the Cu^{2+} ions in the presence of H_2O molecules approximates octahedral symmetry.

The change of the DI/N values of the spectra (Figs. 5a–5c) with copper concentration of the water solutions is linear and the plot passes through the origin. This confirms the validity of their use for the calibration of the ESR signal from the CuH-ZSM-5 samples saturated with water (2, 19). The estimate of the copper concentration derived from the ESR data gives a value of 0.52–0.56 wt% of Cu^{2+} for all mono- and bicationic samples prepared by impregnation and calcined at 520°C. This is in perfect agreement with the quantity of Cu^{2+} introduced (0.5 wt% Cu). Only for the Cu(0.5)Mg(1.1)ZSM-5 sample this value is slightly lower (0.46 wt% Cu). This is strong evidence that the Cu^{2+}–ESR signals from hydrated samples are associated with *all* the copper introduced by impregnation at the level of 0.5 wt%. The results obtained for the same samples calcined at 750°C (steps 4 and 5 of the heat treatment, Figs. 9–11) confirm that all the cupric ions remain isolated and visible by ESR after saturation with water. Only the local crystal field symmetry of Cu^{2+} is changed by the calcination while all the sites remain accessible to H_2O molecules.

Quantitation of "ESR-visible Cu^{2+}" in the two ion-exchanged samples, calcined at 520 and 800°C in air, gives values of 1.8 and 1.65 wt% for base-pretreated and acid-pretreated samples, respectively. These values are near the limit of exchange for the zeolite ($SiO_2/Al_2O_3 = 50$) of 2.05 wt% Cu, assuming a Cu/Al = 1 stoichiometry in this high SiO_2/Al_2O_3 ratio material. Thus, pretreatment of the parent zeolite by base or acid decreases slightly the amount of exchangeable cationic positions with the effect of acidic treatment being a little bit more pronounced. In any case, formation of aggregated copper species is of minor importance, and the majority of copper introduced remains well isolated and contributes to the Cu^{2+}–ESR signal. The fact that in the samples used in our work the Cu^{2+}–ESR signal is associated with virtually all the copper introduced makes the ESR results much more valuable.

(2) Stabilization of square-planar Cu^{2+} sites. Figure 6 shows the ESR spectra of evacuated samples (a) Cu(0.5) ZSM-5, (b) exchCu(1.65)ZSM-5, and (c) Cu(0.5) Mg(1.1) ZSM-5 prepared from the same acid-pretreated zeolite and calcined at 520°C for 3 h (step 1 of the thermal treatment). The results agree with those obtained earlier (1–3, 7, 15–17) and show the presence of the two main configurations, square-planar and square-pyramidal, typical of CuH-ZSM-5 calcined at 500–550°C. The numerical values of the spectral parameters are given in Refs. (15, 17).

Stepwise calcination of the samples in air at increasingly severe conditions (step 2, 650°C, 1 h; step 3, 650°C, 4 h; step 4, 750°C, 1 h; step 5, 750–760°C, 4 h; Step 6, 800°C, 2 h) causes a gradual transformation of Cu^{2+} ESR signals. The spectra from the above-mentioned three samples are shown in Fig. 7, after step 4. The difference in the shape of ESR lines caused by the calcination of the samples is clearly seen from comparison of the two sets of spectra (Figs. 6a and 7a, for example). The structural rearrangement of isolated Cu^{2+} sites occurs without aggregation or encapsulation of the cupric ions but with a gradual irreversible loss of the reactive square-planar sites (1, 3). For better evaluation of the changes in the ESR signals we use an approach proposed earlier (3, 18) and monitor in more detail the $g_{\parallel}$-part of the spectrum. On Figs. 8–11, this part of the signals is magnified to show the details. A cursory, visual comparison of the spectra demonstrates that an identical treatment of different samples causes different changes in the disappearance of Cu^{2+} ions located in square-planar coordination. To monitor quantitatively the loss of this the most reactive part of Cu^{2+} cations, the components of the signal from square-planar Cu^{2+} ions are marked ($g_{\parallel}^{\text{square-planar}} = 2.28$) in the figures, and the most resolved component of this signal is shown by an arrow. The intensity of this line, measured as the line height after baseline correction and signal normalization by weight, copper concentration, and attenuation, is taken as the relative concentration of square-planar Cu^{2+} (3).

Figures 12–14 summarize all the data obtained, showing the relative concentration of the square-planar Cu^{2+} in different samples after stepwise calcination. Low-copper samples, with 0.5 wt% Cu (calculated Cu/Al ratio ~ 0.24) introduced in H-ZSM-5 after the removal of extralattice Al-species by basic or acidic treatment, show no inhibition of the irreversible loss of the most active square-planar sites upon thermal treatment, as compared with the sample

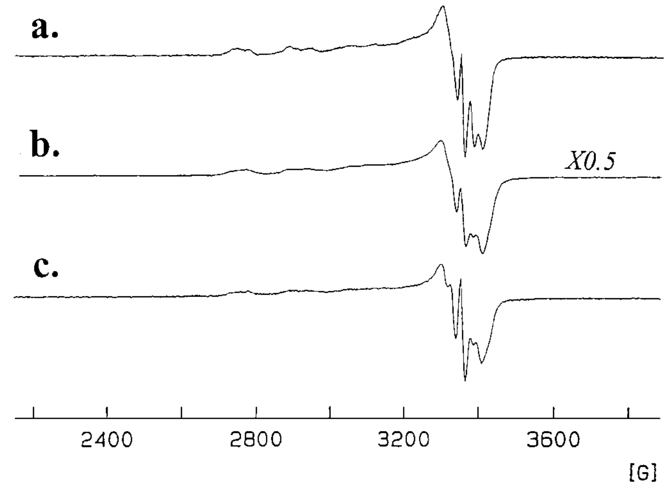

FIG. 6. ESR spectra, at 20°C, of evacuated samples (a) Cu(0.5) HZSM-5, (b) exchanged Cu(1.65)ZSM-5, and (c) Cu(0.5) Mg(1.1)ZSM-5 all on acid-treated zeolite, calcined at 520°C for 2 h (step 1).

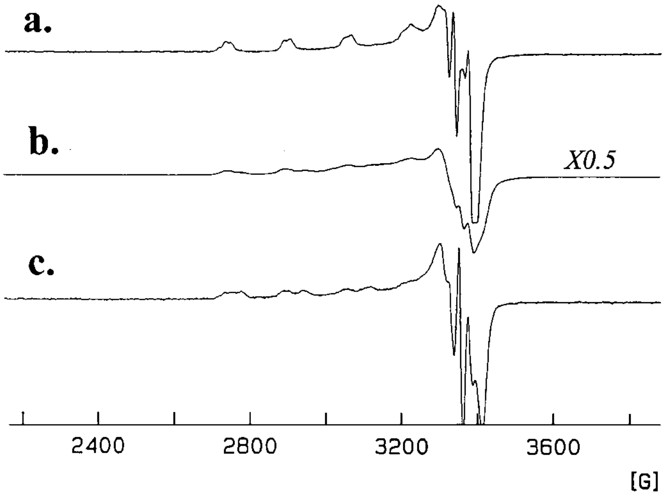

FIG. 7. ESR spectra, at 20°C, of evacuated samples (a) Cu(0.5) HZSM-5, (b) exchanged Cu(1.65)ZSM-5, and (c) Cu(0.5) Mg(1.1)ZSM-5 all on acid-treated zeolite, calcined at 750°C for 1 h (step 4).

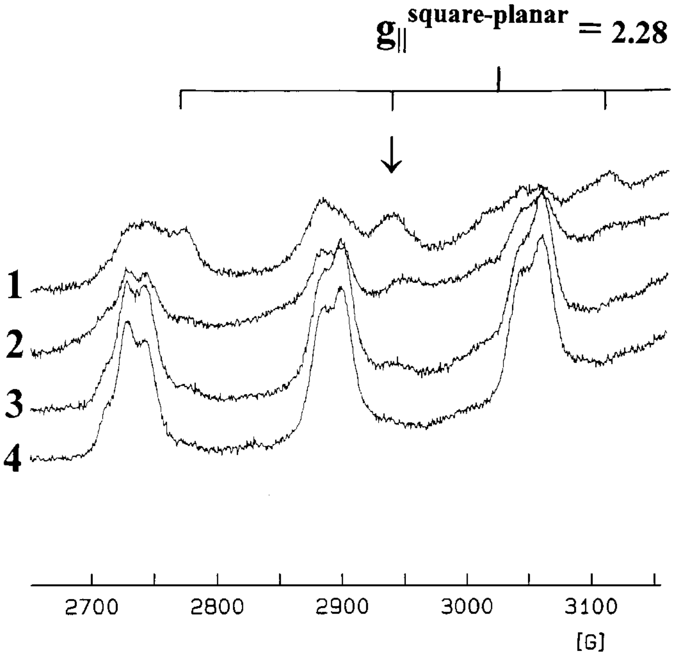

FIG. 8. Changes in the $g_{||}$-part of ESR spectra (20°C) caused by stepwise calcination of the Cu(0.5)HZSM-5 sample: (1) 520°C, 2 h; (2) 650°C, 1 h; (3) 650°C, 4 h; (4) 750°C, 1 h.

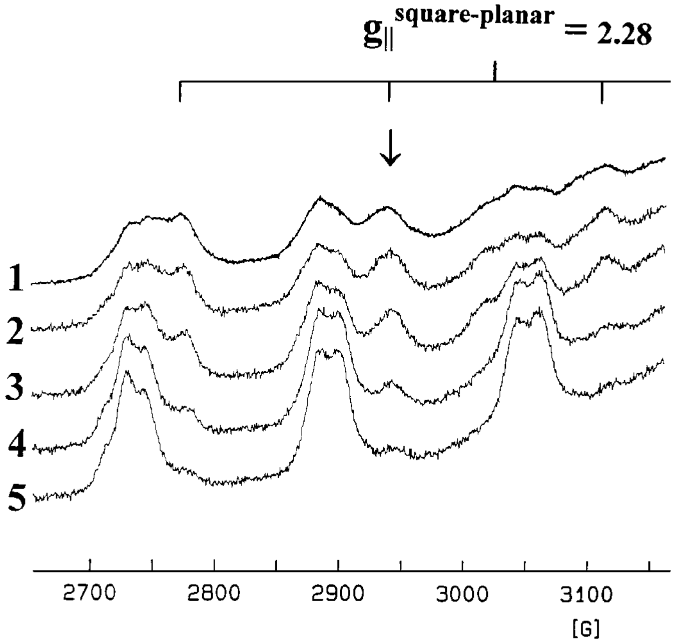

FIG. 10. Changes in the $g_{||}$-part of ESR spectra (20°C) caused by stepwise calcination of the Cu(0.5)La(3.0)ZSM-5 sample: (1) 520°C, 2 h; (2) 650°C, 1 h; (3) 650°C, 4 h; (4) 750°C, 1 h; (5) 750–760°C, 4 h.

prepared from parent zeolite (Fig. 12). However, the same treatment with subsequent *complete* exchange of all Brønsted groups for Cu^{2+} cations (as confirmed by IR data presented on Figs. 3, 4) results in noticeable stabilization of the reactive square-planar sites, as compared with CuHZSM-5 samples having residual protonic sites (Figs. 8, 9, and 12). It is evident that one part of Cu^{2+} ions which exchanges the last portion of the original protons inhibits the irreversible loss of another portion of Cu^{2+}. It is well

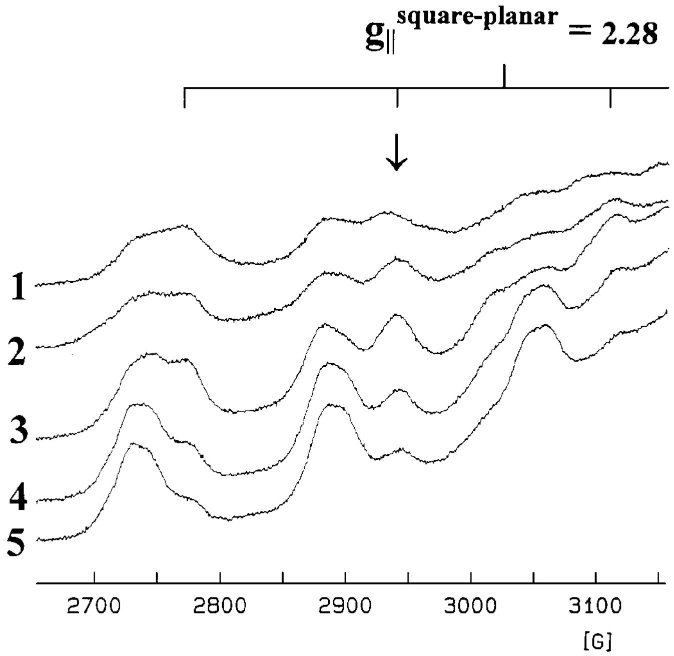

FIG. 9. Changes in the $g_{||}$-part of ESR spectra (20°C) caused by stepwise calcination of the Cu(1.65)HZSM-5 sample: (1) 520°C, 2 h; (2) 650°C, 1 h; (3) 650°C, 4 h; (4) 750°C, 1 h; (5) 750–760°C, 4 h.

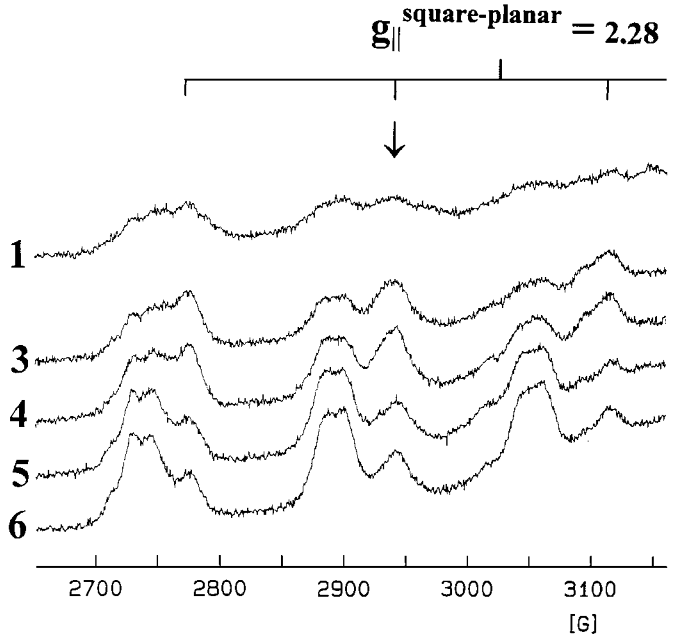

FIG. 11. Changes in the $g_{||}$-part of ESR spectra (20°C) caused by stepwise calcination of the Cu(0.5)Mg(1.1)ZSM-5 sample: (1) 520°C, 2 h; (2) 650°C, 1 h; (3) 650°C, 4 h; (4) 750°C, 1 h; (5) 750–760°C, 4 h.

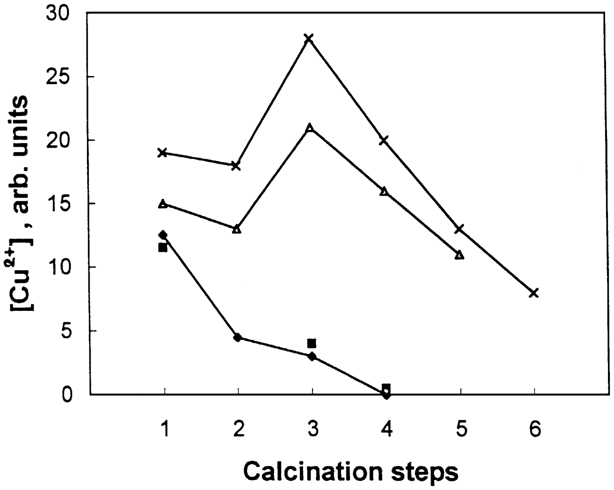

FIG. 12. Relative concentration of square-planar Cu^{2+} after stepwise calcination: (1) 520°C, 2 h; (2) 650°C, 1 h; (3) 650°C, 4 h; (4) 750°C, 1 h; (5) 750–760°C, 4 h; (6) 800°C, 1 h. ◆, Cu(0.5)HZSM-5; ■, Cu(0.5)HZSM-5–HNO$_3$; △, Cu(1.8)ZSM-5–NaOH; ×, Cu(1.8)ZSM-5–HNO$_3$.

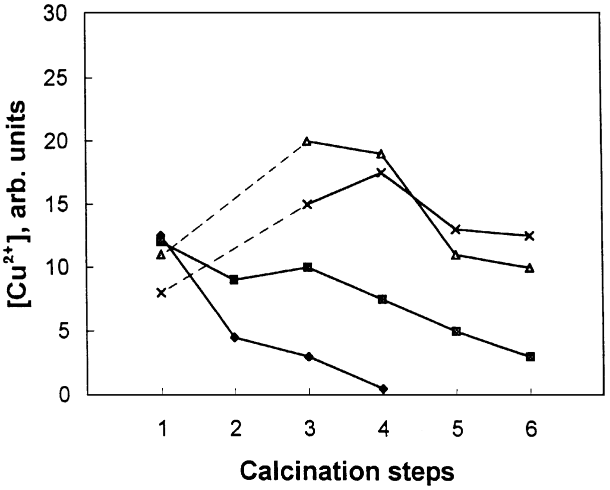

FIG. 14. Relative concentration of square-planar Cu^{2+} after stepwise calcination: (1) 520°C, 2 h; (2) 650°C, 1 h; (3) 650°C, 4 h; (4) 750°C, 1 h; (5) 750–760°C, 4 h; (6) 800°C, 1 h. ◆, Cu(0.5)HZSM-5; ■, Cu(0.5) La(3.0)ZSM-5; △, Cu(0.5)Mg (0.52)ZSM-5; ×, Cu(0.5) Mg(1.1)ZSM-5.

known that H-forms of different zeolites are, in general, less thermally stable than proton-free zeolites. Hence, replacement of the protons in all "weak" sites by cations increases considerably the thermal stability of the system as a whole.

The stabilizing effect of 0.52 wt% Mg, 0.86 wt% Ca, and 1.9 wt% Sr in Cu(0.5)ZSM-5 prepared by impregnation of the base-treated zeolite is shown on Fig. 13. The amount of these elements was chosen to provide an identical atomic concentration of the stabilizing cation. For these bicationic samples (as well as for the sample containing 3.0 wt% La) the calculated ratio [Cu + Me]/Al is ~0.9 (for an idealized zeolite without extralattice Al^{3+}). If the pretreatment of the parent zeolite extracts ~10% of Al, this ratio approaches 1.0. A stabilizing effect is noted for all three elements, with the Mg-containing sample being the most stable. The introduction of the alkaline earth divalent cations to replace the protons substantially retards the rearrangement of the square-planar Cu^{2+} sites into a less reactive state having a higher symmetry of the local crystal field.

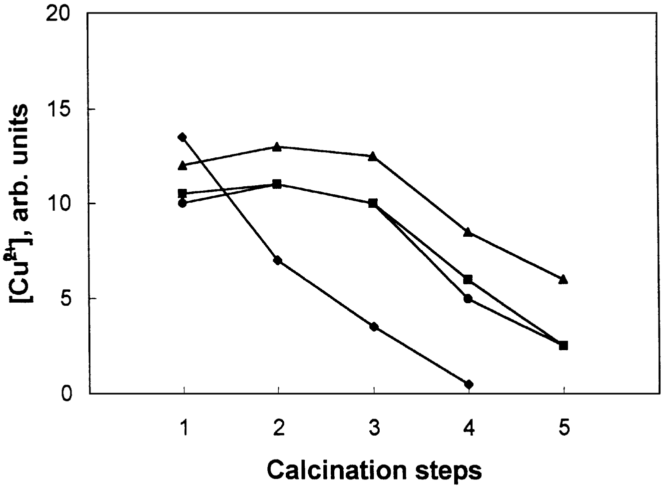

FIG. 13. Relative concentration of square-planar Cu^{2+} after stepwise calcination: (1) 520°C, 2 h; (2) 650°C, 1 h; (3) 650°C, 4 h; (4) 750°C, 1 h; (5) 750–760°C, 4 h. ◆, Cu(0.5)HZSM-5; ■, Cu(0.5)Ca(0.86)ZSM-5; ▲, Cu(0.5)Mg(0.52)ZSM-5; ●, Cu(1.9)Sr(0.52)ZSM-5.

In samples prepared on acid-pretreated zeolite containing 0.5 wt% Cu and 0.55 or 1.1 wt% Mg (Fig. 14) a large part of the copper ions (>50%) preserves the parent square-planar Cu^{2+} state even after calcination at a temperature as high as 800°C. It was shown earlier that La or Ce, when added in sufficient amount, markedly attenuates the spatial rearrangement of the cupric ions during high-temperature calcination of CuLaZSM-5 (3, 6). Therefore, the data for the Cu(0.5) La(3.0)/ZSM-5 are also shown on Fig. 14 for comparison. A pronounced inhibition of the high-temperature reconstruction of Cu^{2+}-sites in CuLaZSM-5 is observed, as compared with the monocationic CuZSM-5. At the same time it is apparent that the stabilization of the CuZSM-5 system by Mg exceeds that provided by La. The combination of the acidic pretreatment with an appropriate amount of Mg^{2+} ions assures the optimal stabilization of the most reactive part of Cu^{2+} cations in CuMgZSM-5.

Magnesium ions compete with Cu^{2+} for the cationic positions but at first the substitution of the less reactive, pyramidal Cu^{2+} cations takes place. Starting at a calcination temperature of 520°C, with further stepwise calcination these samples show an increase in the number of square-planar Cu^{2+} ions after treatment at 650°C; only a more severe heat treatment results in a gradual decrease of the concentration of these ions. An increase in the Mg^{2+} loading to 1.1 wt% (i.e., above the value of one divalent ion per one Al^{3+})

results in a decrease in the number of the reactive cupric sites in the sample calcined at 520°C (step 1) but also further increases the thermal stability (Fig. 14). It seems that the Cu^{2+} ions are bonded in the cationic positions of HZSM-5 somewhat stronger than the Mg^{2+} ions, being able, at higher temperatures to replace the latter with the formation of ESR-active square-planar entities.

CONCLUSION

By removing extralattice Al and completely exchanging the protons in HZSM-5 it is possible to markedly stabilize the tetrahedrally coordinated Cu^{2+} ions when heating in ambient air, containing a few percent moisture. The kind of ion exchanged for the majority of the protons does affect the stability. Optimal stabilization was obtained when Mg^{2+} was used as the modifying ion.

REFERENCES

1. Kucherov, A. V., Hubbard, C. P., and Shelef, M., *J. Catal.* **157**, 603 (1995).
2. Kucherov, A. V., Gerlock, J. L., Jen, H.-W., and Shelef, M., *Zeolites* **15**, 9 (1995).
3. Kucherov, A. V., Hubbard, C. P., Kucherova, T. N., and Shelef, M., *Appl. Catal. B* **7**, 85 (1996).
4. Sano, T., Suzuki, K., Shoji, H., Ikai, S., Okabe, K., Murakami, T., Shin, S., Hagiwara, H., and Takaya, H., *Chem. Lett.* 1421 (1987).
5. Suzuki, K., Sano, T., Shoji, H., Murakami, T., Ikai, S., Shin, S., Hagiwara, H., and Takaya, H., *Chem. Lett.* 1507 (1987).
6. Kucherov, A. V., Hubbard, C. P., Kucherova, T. N., and Shelef, M., *Stud. Surf. Sci. Catal.* **105B**, 1469 (1997).
7. Kucherov, A. V., Gerlock, J. L., Jen, H.-W., and Shelef, M., *Zeolites* **15**, 15 (1995).
8. Kotrla, J., Kubelkova, L., Lee, C.-C., and Gorte, R. J., *J. Phys. Chem. B* **102**, 1437 (1998).
9. Pelmenshchikov, A. G., van Santen, R. A., Janchen, J., and Meijer, E., *J. Phys. Chem.* **97**, 11071 (1993).
10. Pelmenshchikov, A. G., van Wolput, J. H. M. C., Janchen, J., and van Santen, R. A., *J. Phys. Chem.* **99**, 3612 (1995).
11. Szanyi, J., and Paffett, M. T., *J. Chem. Soc. Faraday Trans.* **92**, 5165 (1996).
12. Kucherov, A. V., and Slinkin, A. A., *Kinet. Katal.* **38**, 768 (1997).
13. Chen, J., Thomas, J. M., and Sankar, G., *J. Chem. Soc. Faraday Trans.* **90**, 3455 (1994).
14. Angell, C. L., and Howell, M. V., *J. Phys. Chem.* **73**, 2551 (1969).
15. Kucherov, A. V., Slinkin, A. A., Goryashenko, S. S., and Slovetskaya, K. I., *J. Catal.* **118**, 459 (1989).
16. Kucherov, A. V., Gerlock, J. L., Jen, H.-W., and Shelef, M., *J. Catal.* **152**, 63 (1995).
17. Kucherov, A. V., Gerlock, J. L., Jen, H.-W., and Shelef, M., *J. Phys. Chem.* **98**, 4892 (1994).
18. Larsen, S. C., Aylor, A., Bell, A. T., and Reimer, J. A., *J. Phys. Chem.* **98**, 11533 (1994).
19. Kucherov, A. V., Karge, H. G., and Schloegl, R., *Microporous Mesoporous Mater.* **25**, 7 (1998).